

# NON-UNIFORM HEAVY-ION BEAM TARGET INTERACTIONS

C. K. CHOI, D. B. KOTHE† and M. CHOI

*Purdue University, School of Nuclear Engineering, West Lafayette, IN 47907–1290,  
U.S.A.*

*(Received 20 December 1990)*

The stability and symmetry of a direct-driven inertial confinement fusion (ICF) target irradiated by a heavy-ion beam is studied in planar geometry. Non-uniformities consisting of target surface perturbations (stability) and beam intensity perturbations (symmetry), causing highly distorted flows in the target absorption layers, are considered. The two-dimensional, two-temperature numerical hydrodynamic model FLIP (Fluid-Implicit-Particle), was developed to analyze the beam-driven target implosions. Perturbation amplitudes obtained with FLIP indicate that perturbation wavelengths close to the target shell thickness result in the largest implosion asymmetries.

## 1 INTRODUCTION

The main purpose of this study is to understand the hydrodynamic response of a direct driven planar heavy-ion ICF target which undergoes non-uniform heating by high-intensity ion beams. The physics included in the numerical model comprises 2-d compressible hydrodynamics, 2-T energy transport for electrons and ions, average charge states (Saha relation), Sesame equation of state with equilibrium mix, and the ion beam energy deposition with a unified slowing-down theory. Radiation transport is not included in the model. Neither are atomic-physics processes that are not in local thermodynamic equilibrium (LTE). Burn physics and convergence effects are also neglected, as the hydrodynamic response to perturbations in target material interfaces and beam intensities is the primary emphasis of this study.

A simplifying planar rather than spherical geometry is adopted which is in many cases justified for the early implosion stage. Convergent effects in spherical geometries are likely to amplify any perturbations in planar geometry. The problem is attacked from both a stability and symmetry point of view. The stability point of view is to study the effects of a uniform deposition layer on an initially perturbed target (Figure 1a), while the symmetry point of view is to study the effects of a non-uniform beam deposition layer on an initially smooth target (Figure 1b). The actual situation is, of course, a combination of the two, but the effects are studied separately in hopes of singling out their contributions.

---

† Present Address: Los Alamos National Laboratory, Theoretical Division, Los Alamos, NM 87545.

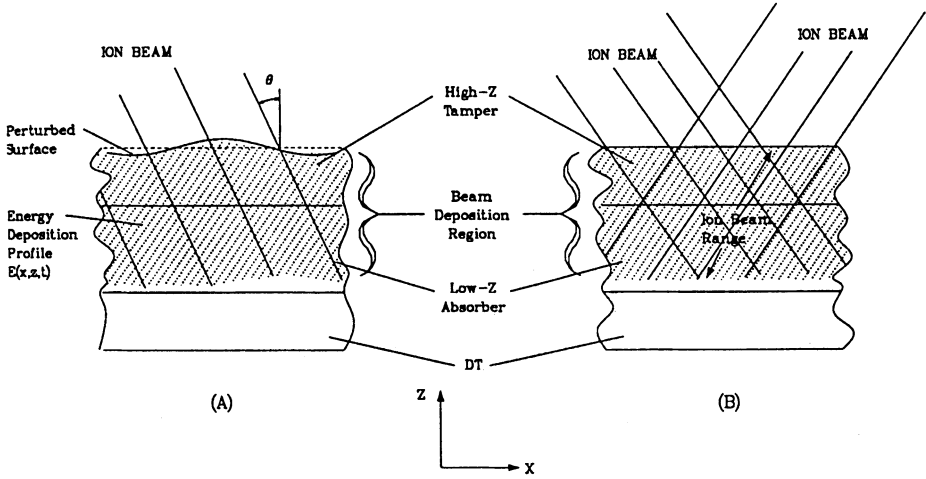


FIGURE 1 Planar model of an ion beam-driven ICF target: (a) uniform beam deposition on an initially perturbed target, and (b) non-uniform beam deposition on an initially smooth target. This planar target has configurations relevant to the HIBALL target<sup>1</sup>.

## 2 PHYSICS AND SIMULATIONS OF BEAM-DRIVEN TARGET IMPLOSION

The hydrodynamics, energy transport, and equations of state for the target plasmas are described in Equations (1) through (7):

$$\frac{d\rho}{dt} = -\rho \nabla \cdot \mathbf{V}, \quad (1)$$

$$\rho \frac{d\mathbf{V}}{dt} = -\nabla p, \quad (2)$$

$$\rho \frac{d\varepsilon_i}{dt} = \nabla \cdot (\kappa_i \nabla T_i) + \omega_{ei}(T_e - T_i) - p_i \nabla \cdot \mathbf{V} + \mu \Phi + \lambda (\nabla \cdot \mathbf{V})^2 + S_i, \quad (3)$$

$$\rho \frac{d\varepsilon_e}{dt} = \nabla \cdot (\kappa_e \nabla T_e) - \omega_{ei}(T_e - T_i) - p_e \nabla \cdot \mathbf{V} + S_e, \quad (4)$$

$$p = p_i + p_e, \quad p_e = p_e(\rho, \varepsilon_e), \quad p_i = p_i(\rho, \varepsilon_i), \quad (5)$$

$$\varepsilon = \varepsilon_i + \varepsilon_e, \quad T_e = T_e(\rho, \varepsilon_e), \quad T_i = T_i(\rho, \varepsilon_i), \quad (6)$$

$$\rho = n_e m_e + n_i m_i = n_i (\bar{Z} m_e + m_i), \quad n_e = \bar{Z} n_i, \quad (7)$$

where  $\rho$  and  $\mathbf{V}$  are the density and velocity of the fluid, respectively. Since discontinuous solutions are not allowed in the transport of momentum, an artificial viscosity is added to the pressure gradient term in Eq. (2) in regions of compression such as shocks in the flow. Eqs. (3) and (4), the specific internal energies for ions and electrons, include thermal diffusion (with diffusivities  $\kappa_i$  and  $\kappa_e$ ), collisions (with collision

frequency  $\omega_{ei}$ ),  $pdV$  work (with ion and electron pressures  $p_i$  and  $p_e$ ), viscous dissipation (with coefficients of a shear viscosity  $\mu$  and bulk viscosity  $\lambda$ , and a dissipation function  $\Phi$ ). There is also an arbitrary source (beam-plasma energy exchanges  $S_i$  and  $S_e$ ),

$$S_{i(e)}(x) = \frac{I(x)}{E(x)} \left( \frac{dE(x)}{dx} \right)_{i(e)},$$

where  $I(x)$  is beam intensity, and  $E(x)$  and  $dE(x)/dx$  are ion beam energy and energy loss per unit path length, respectively. Separate energy transport for the ions and electrons requires separate ion and electron equations of state (EOS) in order to close the system of conservation equations. The SESAME EOS data library from the Los Alamos National Laboratory<sup>2</sup> is used. Energy loss,  $dE/dx$ , to free electrons and plasma ions is described by a unified theory that includes both friction and diffusion in velocity space<sup>3</sup>. This unified formalism, which combines both the binary collision and collective wave phenomena, is capable of handling an arbitrary stopping medium (electrons or ions) without introducing the Coulomb logarithm, and thus is valid for all interaction ranges.

Conventional numerical approaches (Lagrangian or Eulerian) can not accurately model the physics of distorted flows, and thus the Particle-in-Cell (PIC) model<sup>4</sup> for fluid flow needs to be revisited. However, the original (or "classical") PIC has its shortcomings; it is noisy, and it has higher numerical viscosity and heat conduction than would be acceptable today<sup>5</sup>. Many improvements of the "classical" PIC model have been made recently in an algorithm known as FLIP<sup>6</sup>, which eliminates the numerical viscosity and thermal conduction by using a full Lagrangian representation of the fluid (i.e., each particle is attributed all of the properties of the fluid including momentum and energy). The present fluid model for heavy-ion beam-plasma interactions, FLIP-PHD (PlasmaHydroDynamics)<sup>7,8</sup> is based on the FLIP model for fluid flow with the following characteristics: (1) Electric and magnetic fields are neglected; (2) plasmas are assumed to be collisional; (3) ions dominate momentum transport and electrons dominate energy transport; (4) ion beam energy is partitioned differently between plasma ions and electrons, forcing  $T_e \neq T_i$ ; and (5) partial ionization and non-ideal gas EOS are included.

Both zero- and one-dimensional simulations have been performed by FLIP<sup>7</sup> with the proton beam on aluminum foil. The pressure profiles as function of time from the zero-dimensional model of Evans<sup>9</sup>, and the simulations by FLIP were compared for both 15  $\mu\text{m}$  and 30  $\mu\text{m}$  thick aluminum foils that were irradiated by a 16-TW/cm<sup>2</sup>, 1-MeV proton beam with the average range of 2.8 mg/cm<sup>2</sup>.<sup>10,11</sup> The model predicts reasonably well the initial rise in pressure as well as the approximate maximum, calculated by FLIP for 15- $\mu\text{m}$  foil, but breaks down thereafter when a rarefaction propagates back through the foil. When a 30  $\mu\text{m}$  foil, twice as thick as the original thickness, was simulated, a smaller pressure drop was found. This observation explained the original discrepancy that was due to the uniform density assumption made by Evans, and suggested that the agreement between the models was good.

The proton-foil interaction recently studied at the Naval Research Laboratory<sup>10</sup>

was compared with the FLIP calculation for 1-D planar implosion<sup>7</sup>. The FLIP calculation used 50 zones with 16 particles per cell and incorporated physics discussed in this section. The grid boundary was allowed to move with a semi-Lagrangian in order to follow the expansion of foil. Temperature, density, and energy deposition profiles are compared and they represent the same functional behavior with some numerical discrepancies, which were caused mainly by using different stopping power theories.

### 3 2-D STABILITY AND SYMMETRY ANALYSIS FOR NON-UNIFORM TARGETS

The “planar” HIBALL (Heavy Ion Beams And Lithium Lead)<sup>1</sup> target configuration (i.e., single-shell, multilayered target with an infinite radius as in Figure 1) was chosen for this assessment since it currently represents the prototype design of a target to be imploded by direct driven heavy-ion beams in future ICF reactors. The planar target consists of a tamper layer of lead ( $\Delta_{\text{Pb}} = 140 \mu\text{m}$ ), an absorber/pusher layer of lithium seeded with lead ( $\Delta_{\text{LiPb}} = 500 \mu\text{m}$ ), and cryogenic liquid DT fuel layer ( $\Delta_{\text{DT}} = 155 \mu\text{m}$ ). Since convergence effects are not modeled here, the void on the inner side of the DT layer will be treated as an infinite vacuum in planar geometry. The 10 GeV  $\text{B}_i^+$  ions depositing 4.37 MJ of energy in the target with 4 mg of cryogenic DT over a period of 30 ns are considered to simulate a HIBALL-like target. This design grew from a design originally proposed by Bangerter and Meeker<sup>12</sup>, which to date remains the generic single-shell design (tamper, absorber/pusher, and fuel layer) for ion-driven ICF targets.

Two cases of perturbed non-uniform beam-target interactions are considered; Case I, the perturbation on target surface for stability studies, and Case II, the perturbed incoming ion beams for symmetry analyses. Case I corresponds to the implosion phase of a non-uniform planar target initially having a single-mode Pb/LiPb surface perturbation, with target thickness  $795 \mu\text{m}$ , and dimensionless wave number  $kd = 20$ . The target is uniformly irradiated for 30 ns by a normally incident, 10 GeV  $\text{B}_i^+$  beam with an intensity  $I_0$  equal to  $1 \text{ TW}/\text{cm}^2$ . Case II is related to a uniform planar target driven for 30 ns by a normally incident, 10 GeV  $\text{B}_i^+$  perturbed beam having an intensity variation  $I(x, t) = I_0(t) [1 + a \cos(kx)]$ , where  $x$  is defined in the lateral direction of the target with  $0 \leq x \leq 120 \mu\text{m}$ ,  $I_0 = 1 \text{ TW}/\text{cm}^2$ ,  $a = 0.05$ , and  $kd = 20$ .

Figure 2 shows the results of the time history of various perturbation amplitudes in Case I. The density perturbation amplitudes in Figure 2 deviate from a straight line, indicating a departure from linear growth (at an amplitude-to-wavelength ratio of about 0.2). This result is in qualitative agreement with the simulations of laser-driven, ablatively accelerated thin shells by Verdon *et al.*<sup>13</sup>. They found that Rayleigh–Taylor (R–T) bubble growth is the primary cause of shell rupture. A more realistic spherical target having a Pb/LiPb surface perturbation similar to the one imposed in this implosion, admittedly severe and larger than fabrication tolerances, would most likely fail to ignite.

Computational results for Case II are also illustrated in Figure 3. It shows the

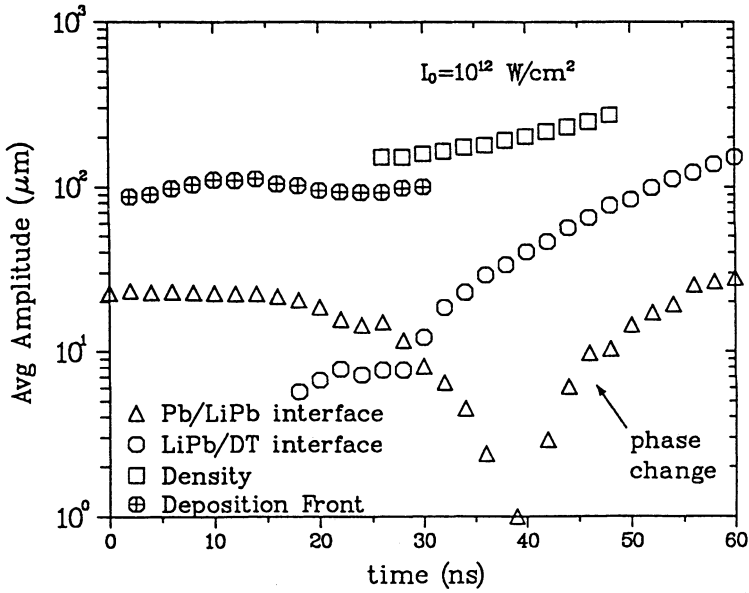


FIGURE 2 Computed average perturbation amplitudes (one-half of the peak-to-valley value) of various quantities versus time for a uniform  $1 \text{ TW/cm}^2$  irradiation on the planar target having an initially imposed Pb/LiPb surface perturbation of amplitude  $22.5 \mu\text{m}$  and wavelength  $240 \mu\text{m}$ .

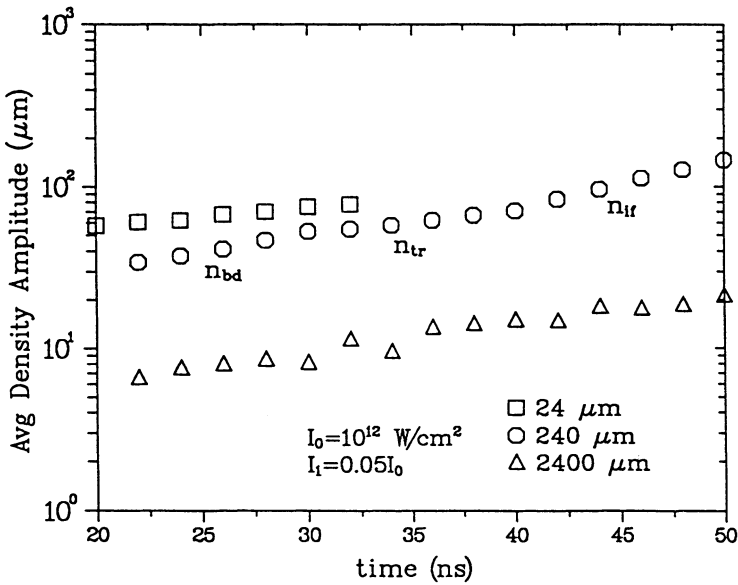


FIGURE 3 Computed average perturbation amplitudes (one-half of the peak-to-valley value) of density of a uniform planar target for three beam intensity perturbation wavelengths, each with a 5% amplitude about  $1 \text{ TW/cm}^2$ .

pattern of density amplitude growth with three distinct slopes visible through the points denoting growth rates  $n_{bd}$  ("beam driven" for 22 to 30 ns),  $n_t$  ("transitional" for 30–40 ns), and  $n_{if}$  ("interfacial" for 40–50 ns). Density amplitudes for  $\lambda = 2400 \mu\text{m}$  are very small, almost at the level of computational noise. The short-wavelength calculation ( $\lambda = 24 \mu\text{m}$ ) is terminated at 32 ns because of problems with the finite grid instability, which rendered the results suspicious at later times. It is apparent in Figure 3 that the maximum density perturbation growth rate occurs at  $\lambda = 240 \mu\text{m}$ .

#### 4 DISCUSSION

The two-dimensional stability and symmetry analysis for non-uniform heavy-ion beam-target interactions was investigated. At low intensities for Case I, surface perturbations at the Pb/LiPb interface appear to be more disastrous than similar perturbations at the LiPb/DT interface because the LiPb/DT interface is beyond the beam ion range. Perturbations at the Pb/LiPb and LiPb/DT interfaces grow in a targets appear to be extremely sensitive to beam non-uniformities, with the target sensitivity going up with the beam intensity. The beam intensity perturbations with wavelengths on the order of payload (i.e., DT plus fraction of LiPb absorber/pusher) shell thickness result in higher implosion asymmetries.

#### REFERENCES

1. B. Badger *et al.*, HIBALL-A Conceptual Heavy Ion Beam Driven Fusion Reactor Study, University of Wisconsin report UWFDM-450 (1981); also, B. Badger *et al.* HIBALL-II—An Improved Heavy Ion Beam Driven Fusion Reactor Study, UWFDM-625 (1984).
2. K. S. Holian, ed., Los Alamos National Laboratory report LA-10160-MS (1984).
3. C. K. Choi and M. Hsiao, *Nucl. Technol./Fusion* **3** 273–279 (1983).
4. F. H. Harlow and M. Evans, "A machine calculation method for hydrodynamics problems," Los Alamos National Laboratory report LAMS-1956 (1955); also, F. H. Harlow, *J. Assoc. Comput. Mach.* **4** 137–142 (1957).
5. A. Nishiguchi and T. Yabe, *J. Comput. Phys.* **52** 390 (1983).
6. J. U. Brackbill and H. M. Ruppel, *J. Comput. Phys.* **65** 314–343 (1986).
7. D. B. Kothe, Ph.D. thesis, Purdue University, 1987.
8. D. B. Kothe, C. K. Choi, and J. U. Brackbill, *Laser Interaction* (ed. by H. Hora and G. Miley) (Plenum, 1988), Vol. 8, pp. 701–721; also, D. B. Kothe, J. U. Brackbill, and C. K. Choi, *Phys. Fluids B* **2** (1990) 1898–1906.
9. R. G. Evans, *Laser and Particle Beams* **1** 231–239 (1983).
10. J. E. Rogerson, R. W. Clark, and J. Davis, *Phys. Rev. A* **31** 3323–3331 (1985).
11. B. P. Goel, G. A. Moses, and R. R. Peterson, *Laser and Particle Beams* **5** 133–154 (1987).
12. R. Bangerter and D. Meeker, "Ion beam inertial fusion target designs," Lawrence Livermore National Laboratory report, UCRL-78474 (1976).
13. C. P. Verdon, R. L. McCrory, R. L. Morse, G. R. Baker, D. I. Meiron, and S. A. Orszag, *Phys. Fluids* **25** 1653–1674 (1982).